Original Research

Age-associated expression of HCN channel isoforms in rat sinoatrial node

Xin Huang[1], Pei Yang[2], Zhao Yang[3], Hong Zhang[4] and Aiqun Ma[1]

[1]Department of Cardiology, First Affiliated Hospital of Xi'an Jiaotong University Health Science Center, Ion Channel Disease Laboratory, Key Laboratory of Environment and Genes related to Diseases of Education Ministry, Xi'an, Shaanxi 710061, P.R. China; [2]Department of Orthopedics, Second Affiliated Hospital of Xi'an Jiaotong University Health Science Center, Xi'an, Shaanxi 710004, P.R. China; [3]Institute of Medical Electronics in Medical School, Key Laboratory of Biomedical Information Engineering, Ministry of Education, Xi'an Jiaotong University, Xi'an, Shaanxi 710061, P.R. China; [4]School of Electrical Engineering, Xi'an Jiaotong University, Xi'an, Shaanxi 710049, P.R. China
Corresponding author: Aiqun Ma. Email: drmaaiqun@163.com

Abstract

The expression of hyperpolarization-activated cyclic nucleotide-gated cation (HCN) channel isoforms varies among species, cardiac tissues, developmental stages, and disease generation. However, alterations in the HCN channels during aging remain unclear. We investigated the protein expressions of HCN channel isoforms, HCN1-HCN4, in the sinoatrial nodes (SANs) from young (1-month-old), adult (4-month-old), and aged (30-month-old) rats. We found that HCN2 and HCN4 proteins were present in rat SAN using immunohistochemistry; therefore, we quantitatively analyzed their expression by Western blot. Aim to correlate protein expression and pacemaking function, specific blockade of HCN channels with 3 μmol/L ivabradine prolonged the cycle length in the intact rat heart. During the senescent process, the HCN2 and HCN4 protein levels declined, which was accompanied with a decreased effect of ivabradine on rat SAN automaticity. These results indicated the age-associated expression and relative function of HCN channel isoforms.

Keywords: Aging, sick sinus syndrome, ion channels, sinoatrial node

Introduction

Sick sinus syndrome (SSS) is commonly seen in the aged population.[1] The aged sinoatrial node (SAN) has a reduced velocity of diastolic and phase 0 depolarization, with a lengthened action potential duration,[2,3] manifesting in a decreased SAN function with a reduced intrinsic heart rate (IHR), prolonged sinoatrial conduction time (SACT), and sinoatrial node recovery time (SNRT).[4] However, the underlying age-associated electrical remodeling of SAN remains uncertain.

Diverse data support a specific role of pacemaker current (I_f) carried by the hyperpolarization-activated cyclic nucleotide-gated (HCN) cation channel in pacemaking and heart rate control. The specific HCN channel blocker, ivabradine, acting as a "pure heart rate reducing" agent, is used today as a therapeutic tool in chronic stable angina and heart failure.[5] Also, the pacemaking capability of HCN channels has been the main rationale behind the development of "biological" pacemakers, whose aim is to eventually replace the electronic pacemakers implanted today.[6] In human,

HCN dysfunction can result in the genesis of symptomatic sinus bradycardia, tachycardia–bradycardia syndrome, atrioventricular node block, atrial fibrillation, etc. However, the precise expression and function of each HCN channel isoform related to physiology and pathology remain debated.

The mammalian genome encodes four HCN channels, that is HCN1–HCN4, which share ~80% of homology and differ mainly in activation kinetics and sensitivity to cAMP.[7–10] The expression of these HCN channel isoforms assumes species, developmental, and tissue heterogeneity.[7,11] In adult SAN, HCN4 is the dominant HCN isoform of all species investigated including rabbit, murine, and canine, accounting for ~80% of the total HCN message.[12,13] HCN1 takes up 18% of the total HCN mRNA in rabbit SAN[13] but only at very low level in mouse SAN.[12] HCN2 transcripts are also expressed in mouse SAN. However, they are equally distributed among atria and SAN at a low to moderate level, unlike the dominant distribution of HCN4 transcripts in the nodal region.[12] In addition, the dynamic transcriptions of HCN channel isoforms during normal

cardiac development and disease generation have been revealed. During mouse cardiac development, embryonic atrium and ventricle revealed abundant HCN4 transcription but other HCN transcripts were almost absent. Toward birth, HCN4 was downregulated in the atrium and almost vanished from the ventricle. At postnatal day 10, HCN4 was highest in the SAN, being twofold higher than HCN1 and fivefold higher than HCN2. This developmental and tissue-specific transcription pattern of HCN isoforms may be required to establish and ensure a stable heart rhythm and to prevent atrial and ventricular arrhythmogenesis in adult.[14] In hypertrophied or failing hearts, transcripts of HCN2 and HCN4 were upregulated in working myocardium, which may be related to a higher incidence of arrhythmias.[15,16] All above findings lead to the hypothesis that an age-associated expression of HCN channel isoforms may trigger, at least in part, the declined function of aging SAN.

This set of experiments is aimed to identify the age-associated expression of the HCN channel isoforms at the protein level in rat SAN. Our results indicate that the HCN2 and HCN4 isoforms are expressed in SAN cells, but they are virtually absent in the surrounding atrial myocytes. During the senescent process, the HCN2 and HCN4 protein levels declined, which was accompanied with a decreased effect of ivabradine, a blocker of HCN channel, on rat SAN automaticity.

Materials and methods

Animal preparation

Animal procedures were performed in accordance with the Guide for the Care and Use of Laboratory Animals issued by the Institute of Laboratory Animal Resources (NIH publication 85-23, revised 1996). The study was also approved by *the Xi'an Jiaotong University Animal Care and Use Committee*.

Male Sprague-Dawley rats, which were one (young) and four months old (adult), were obtained from the Xi'an Jiaotong University Laboratory Animal Center, and 30-month-old rats (aged) were purchased from Shanghai Laboratory Animal Center, Chinese Academy Sciences (Shanghai, China). All rats were housed in a temperature-controlled room under a 12 h/12 h light/dark and were allowed access to standard rat chow and tap water *ad libitum*.

SAN function

ECGs were recorded under anesthesia with sodium pentobarbitone (40 mg/kg, *i.p.*, Sigma, USA). The stimuli were applied to the right atrial appendage by a bipolar stimulus through the esophagus. SACT was tested by premature atrial stimulation reported by Strauss *et al.*[17] The stimuli were introduced late in atrial diastole and moved progressively earlier in 3–5 ms increments, until the entire atrial diastolic period was scanned. When the spontaneous sinus cycle was interrupted by an atrial premature depolarization (APD), the following atrial intervals were measured: (1) spontaneous sinus cycle length (CL) (A-A), i.e. the

interval between the last two spontaneous sinus P waves that preceded the APD; (2) the test cycle (A-AT), i.e. the interval between the last spontaneous sinus P wave and the APD; (3) the return cycle (AT-AR), i.e. the interval between the APD and the following spontaneous sinus P wave. Earlier in atrial diastole, not only did progressive shortening of the test cycle (A-AT) fail to result in reciprocal lengthening of the return cycle (AT-AR) but the return cycle duration remained nearly constant. The return cycle was no longer fully compensatory but was greater than one spontaneous sinus cycle (A-A). This change in return cycle response marked the transition from zone I to zone II. Then the difference between AT-AR and A-A reflects conduction time into and out of the SAN. The SACT was calculated to be approximately the product of one half the distance. SNRT was obtained by 30 s of overdrive pacing, beginning at a frequency of 6.5 Hz, with a 0.5 Hz increment, until the SNRT was no longer lengthened.[18] The longest time interval from the last paced atrial depolarization to the first spontaneous sinus cycle was designated as the SNRTmax. The rate-corrected maximal sinoatrial node recovery time (CSNRTmax) was determined by subtracting the spontaneous sinus cycle from the SNRTmax.

The IHR in vivo

The IHR was tested under complete blockade of the cardiac autonomic nervous system with propranolol (3 mg/kg/mL i.v., Sigma, USA) and atropine (2 mg/kg/mL i.v., Sigma, USA) as previously reported.[19] Additionally, the IHR was recorded and averaged for 1 min.

The CL in Langendorff hearts

Excised hearts were quickly mounted on a Langendorff apparatus at a constant pressure of 80 mmHg with warm ($36 \pm 0.5°C$), oxygenated, modified Krebs–Henseleit bicarbonate (KHB) buffer as described previously.[20] The composition of the modified KHB was as follows: (in mmol/L) NaCl 118, KCl 4.7, $MgSO_4$ 1.2, KH_2PO_4 1.2, glucose 11.0, $CaCl_2$ 2.0, pyruvate 2.0, $NaHCO_3$ 25, and insulin 5 U/L (PH 7.4 ± 0.5). Two recording electrodes were attached to the atrial appendages, and data were sampled with a BL-420 Electrophysiograph (Chengdu Taimeng Technology Co., Ltd, Chengdu, Sichuan, China). Electrocardiographies were recorded at baseline and at the end of 25 min perfusion of 3 μmol/L ivabradine (Sigma, USA) which demonstrated to reduce about 60% I_f without obvious effect on T-type and L-type calcium current and delayed rectifier potassium current[21]; subsequently, the ivabradine was washed out with KHB buffer for 25 min. After perfusion, heart samples were removed, blotted dry, and weighed. The CL was averaged over 3 min.

Immunohistochemistry

As previously reported,[22] the leading pacemaker site recognized by optical mapping was isolated, fixed, dehydrated, and embedded in optimal cutting temperature compound (Tissue-Tek, NL). Frozen 10 μm sections were serially cut across the leading pacemaker site perpendicular to the

crista terminalis. Serial sections were labeled with HE and Masson stains, rabbit polyclonal antibodies against connexin 43 (Cx43) (1:2000; Sigma, USA), and the hyperpolarization-activated cyclic nucleotide-gated potassium channel 1-4 (HCN1-4) (1:200; Alomone Labs, Israel), respectively. The FITC-conjugated goat anti-rabbit IgG (Zhongshan Golden Bridge Biotechnology Corporation, Beijing, China) was used as the secondary antibody with a dilution factor of 1:100. For positive control experiments, rat brain tissue was used. For the negative control experiments, the primary antibody was substituted by horse serum (4%) alone. The sections were analyzed under a Leica TCS SP 2 laser scanning confocal microscope (Leica, Germany) in a blinded manner by two senior pathologists from Pathology Department of First Affiliated Hospital of Xi'an Jiaotong University.

Western blot assay

Membrane proteins were extracted from the leading pacemaker site of SAN, by centrifugation on a sucrose buffer (including protease inhibitor cocktail) according to the protocol published by Alomone Labs. Western blot was performed as described previously.[23] The rabbit polyclonal antibodies to rat HCN2 and HCN4 (1:200 dilution, respectively) or mouse monoclonal antibody to rat β-actin (1:2000 dilution, Santa Cruz Biotechnology, Inc., Texas, USA) were used as the primary antibodies. The goat anti-rabbit IRDye® 800CW or goat anti-mouse IRDye® 680 LT secondary antibody (1:2000 dilution) (Li-COR Biosciences, NE, USA) was used as the secondary antibodies. Bands were then detected by using Odyssey for Infrared Fluorescent Western Blots

from Li-COR Bioscience (Lincoln, NE). Quantitative analysis of the Western blot results was performed with the Odyssey software 3.0 (Li-COR Bioscience, Lincoln, Nebraska). For positive control experiments, membrane proteins of rat brain tissue were used. For the negative control experiments, the primary antibody was substituted by phosphate buffered saline alone.

Statistical analysis

Data are expressed as the means $\pm$ SEM. The significance of difference was determined by analysis of variance and a *post hoc* multiple comparison test using the SPSS 11. 0 software. Statistical significance was established at $p < 0.05$.

Results

Age-associated changes of the physical characteristics of SAN

The intrinsic SAN function was examined in three ages of rats, young, adult, and aged, with recording of SACT and CSNRT under autonomic blockage (n = 16 for each age group). Figure 1 shows a representative measurement trace of SACT by atrial premature stimulation through esophagus *in vivo* from the young group. The stimuli were introduced earlier in atrial diastole when progressive shortening of the test cycle (A-AT) failed to result in reciprocal lengthening of the return cycle (AT-AR) but the return cycle duration remained nearly constant. The return cycle was no longer fully compensatory but was greater than one spontaneous sinus cycle (A-A). This change in return cycle response marked the transition from zone I to zone II. Then the difference between AT-AR and A-A reflects conduction
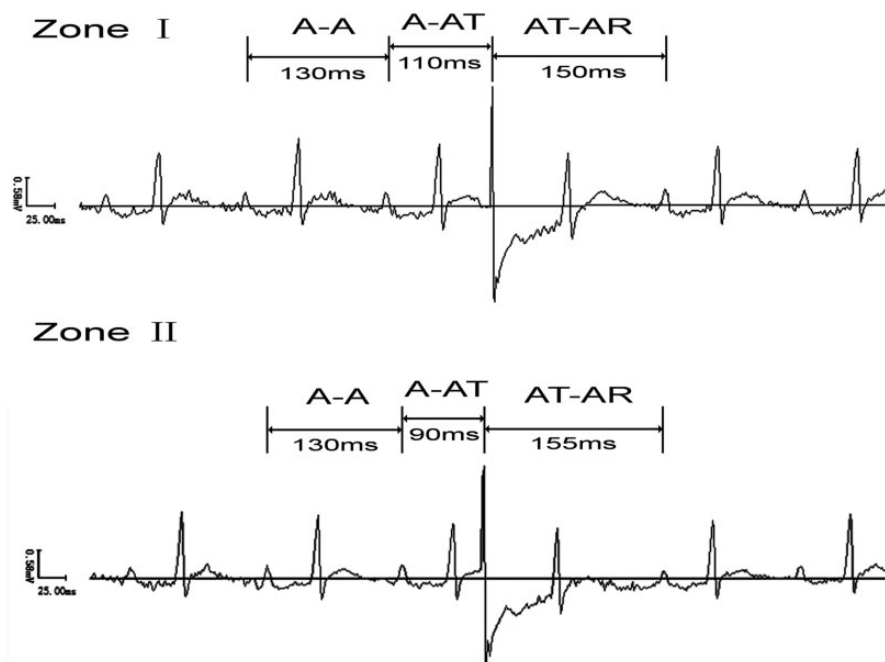

Figure 1 Measurement of sinoatrial conduction time (SACT) by premature atrial stimulation through esophagus *in vivo* (from the young group). The stimuli were introduced earlier in atrial diastole when progressive shortening of the test cycle (A-AT) failed to result in reciprocal lengthening of the return cycle (AT-AR) but the return cycle duration remained nearly constant. The return cycle was no longer fully compensatory but was greater than one spontaneous sinus cycle (A-A). This change in return cycle response marked the transition from zone I to zone II. Then the difference between AT-AR and A-A reflects conduction time into and out of the SAN

time into and out of the SAN. SACT = [(AT-AR)-(A-A)]/2. The SACT and CSNRTmax were significantly lengthened from youth to senescence. The resting heart rate (RHR) and IHR, which reflect the intrinsic SAN activity, were also decreased with increasing age (Table 1).

Age-associated effect of ivabradine on the CL in Langendorff hearts

A pseudo-ECG was recorded from the surface of the left and right atrial appendages (Figure 2(a)). The physiological significance of HCN channels in automaticity was analyzed with the application of ivabradine, which is known to inhibit I_f specifically. Three µmol/L ivabradine significantly prolonged CL by 33.2 ± 2.5, 25.7 ± 2.4, and $12.7 \pm 2.1\%$ in the young, adult, and aged rats, respectively ($p < 0.001$ versus age-matched control group, n = 5) (Figure 2(b)).

Expression of HCN channel isoforms in rat SAN

The rat SAN is located in the posterior wall of the right atrium; a coarse anatomical definition identifies this structure as the intercaval region adjacent to the atrial muscle of the crista terminalis, extending from the superior to near the inferior vena cava (Figure 3(a)). With HE staining, the SAN

Table 1 Age-associated changes of the physical characteristics and the SAN function

Characteristics	Young	Adult	Senescent
BW (g)	50 ± 1.2	$350 \pm 1.5^*$	$500 \pm 4.7^{\#}$
HW (mg)	292 ± 14	$1236 \pm 11^*$	$1797 \pm 15^{\#}$
HBWR (mg/g)	5.91 ± 0.04	$3.36 \pm 0.03^*$	3.52 ± 0.03
RHR (bpm)	530 ± 7	$382 \pm 5^*$	$331 \pm 4^{\#}$
IHR (bpm)	430 ± 4	$310 \pm 2^*$	$255 \pm 5^{\#}$
SACT (ms)	12.5 ± 0.6	$17.7 \pm 0.2^*$	$22.5 \pm 0.4^{\#}$
CSNRT$_{max}$ (ms)	33.9 ± 1.0	$50.7 \pm 3.0^*$	$78.1 \pm 4.9^{\#}$

BW: body weight; CSNRTmax: rate-corrected maximal sinoatrial node recovery time; HBWR: heart-to-body weight ratio; HW: heart weight; IHR: intrinsic heart rate; RHR: resting heart rate; SACT: sinoatrial conduction time.
Mean $\pm$ SEM, n = 16, $^*P < 0.05$ versus young group; $^{\#}P < 0.05$ versus adult group.

cells are small and empty compared to the surrounding atrial cells (Figure 3(b)). Masson staining reveals a heterogeneous architecture with myocytes that are sparsely distributed in a dense connective matrix. A characteristic feature of the SAN is substantial connective tissue, mainly collagen and fibroblasts (Figure 3(c)).

SAN cells lack Cx43. Instead, adjacent atrial working myocytes take on positive staining of Cx43. As illustrated in Figure 4, the SAN tissues have robust HCN2 and HCN4 staining with negative HCN1 and HCN3 staining (data not shown).

Age-associated expression of HCN channel isoforms in rat SAN

The pacemaker activity and activation conduction were recorded by voltage-sensitive fluorescent signals from 64×64 sites simultaneously at a rate of 910 frames/s over the SAN and adjacent atrium (Figure 5). The mapping field was $20\,mm \times 20\,mm$. Only the leading pacemaker site as surrounded by yellow line in Figure 5(d) was harvested for further Western blot assay. As shown in Figure 6, HCN2 and HCN4 in the SAN were further evaluated by Western blot analysis. The protein expression of HCN2 was reduced from 0.74 ± 0.13 in the young rats to 0.51 ± 0.10 in the adult rats and then further decreased to 0.36 ± 0.04 in the aged rats (aged versus young, $p < 0.01$; aged versus adult, $p < 0.05$; n = 20 for each group). Similarly, the HCN4 expression in the SAN was also decreased during aging (from $[0.62 \pm 0.09]$ in the young rats to $[0.47 \pm 0.11]$ in the adult rats and then to $[0.24 \pm 0.09]$ in the aged rats) (aged versus young, $p < 0.01$; aged versus adult, $p < 0.05$; n = 20 for each group).

Discussion

Our results revealed that (1) the presence of HCN2 and HCN4 proteins in the rat SAN and (2) there is an age-associated decline in the expression of HCN2 and HCN4 proteins accompanied with a reduction in their relative contribution to SAN pacemaking.

The normal heart rate is triggered by rhythmic spontaneous depolarization of SAN during the diastole. The
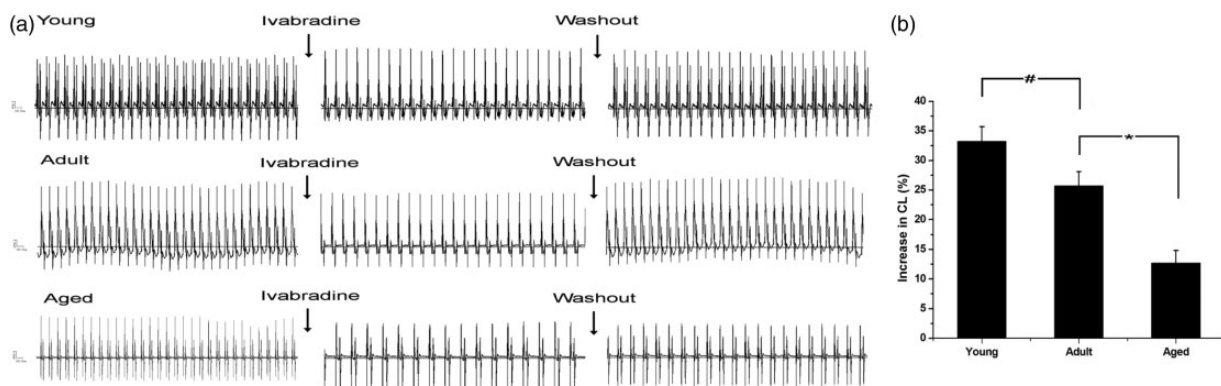

Figure 2 Effect of ivabradine on the cycle length (CL) in Langendorff hearts from the young, adult, and aged rats. (a) Representative electrocardiogram recorded before, during, and after (washout with KHB buffer) 3 µmol/L ivabradine perfusion. (b) Declined effect of ivabradine on CL with age. $^{\#}p < 0.05$ versus the young group; $^*p < 0.001$ versus the adult group; n = 5
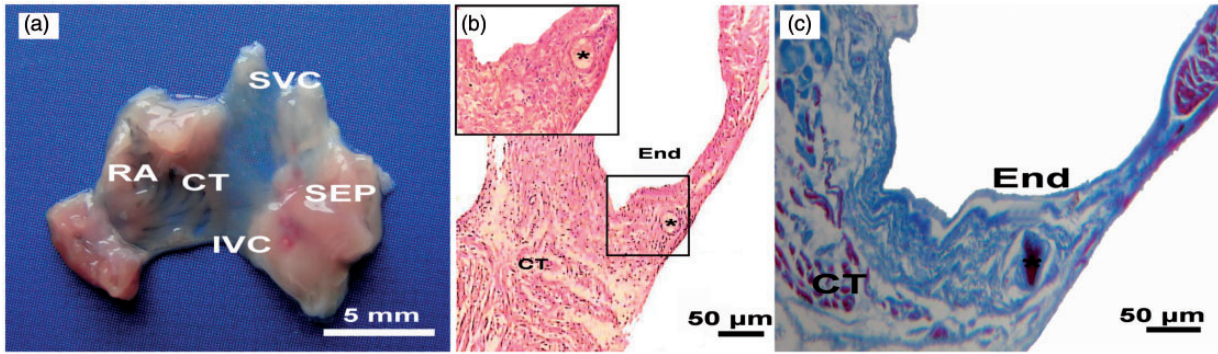
Figure 3 Histology of rat SAN tissue (from the young group). (a) The image of the raw SAN preparation. (b) HE staining of the SAN tissue. (c) Masson staining of the SAN tissue. * indicates SAN artery. CT: crista terminalis; End: endocardium; IVC: inferior vena cava; RA: right atrium; SEP: septum; SVC: superior vena cava. (A color version of this figure is available in the online journal.)
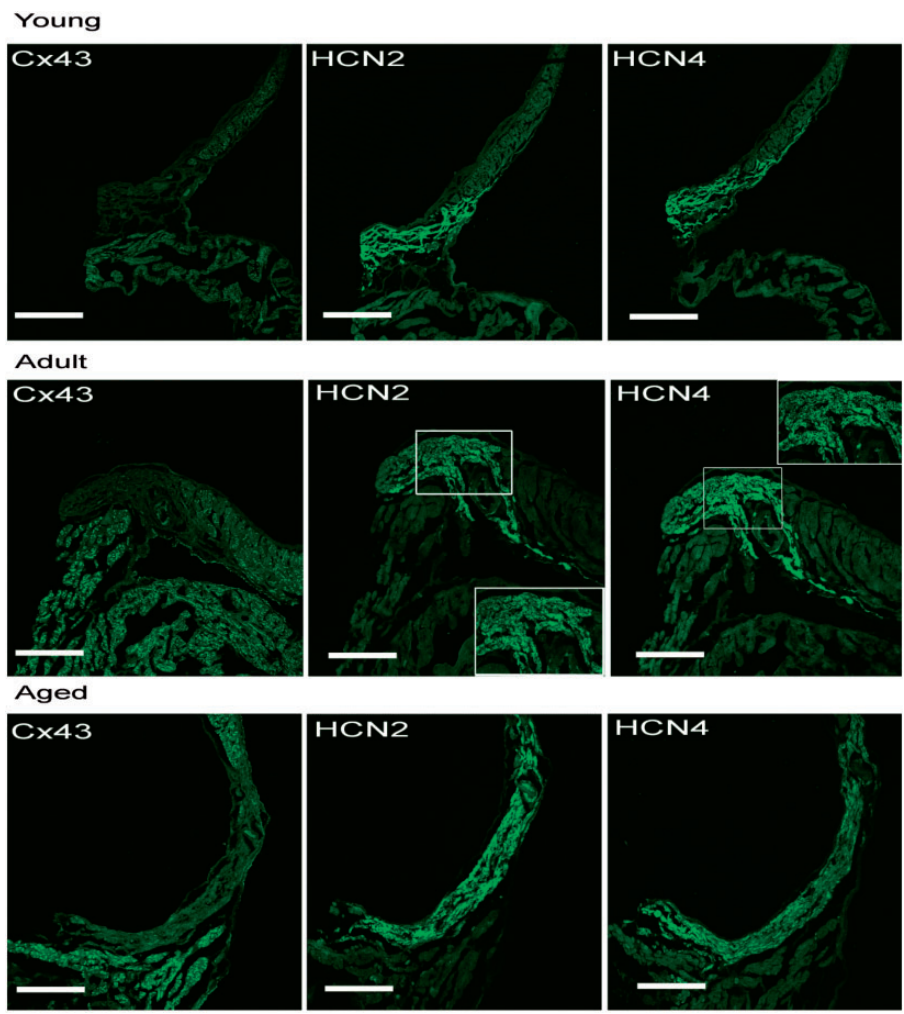

Figure 4 Confocal images of serial sections of SAN tissues labeled with Cx43, HCN2, and HCN4 from the young, adult, and aged rats. SAN tissues have robust HCN2 and HCN4 staining. Scale bar = 300 μm. (A color version of this figure is available in the online journal.)

hyperpolarization-activated cyclic nucleotide-gated cation current, termed I_f, carried by HCN channel, plays a key role in the pacemaker activity.[24,25] To date, four HCN channel isoforms have been identified in the heart. Furthermore, the relevance of each HCN channel isoform to maintaining a stable heart rate and regular beat-to-beat variation has been confirmed in genetic mouse models *in vivo*.[26–29] Mice lacking HCN1 display sinus node dysrhythmia and recurrent sinus pauses pronounced at low heart rates and nearly absent at the high heart rates observed during high physical
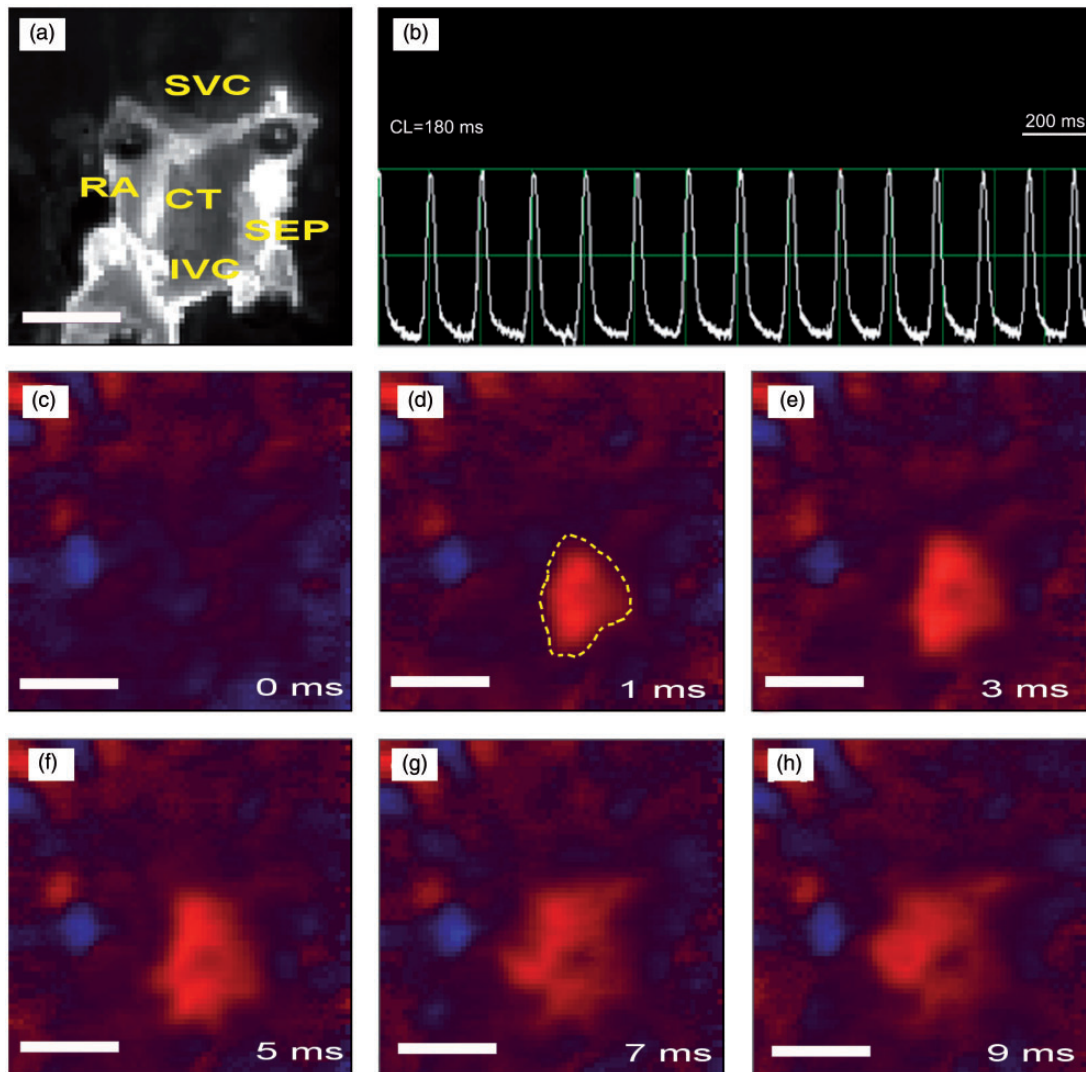
Figure 5 Optical mapping over rat SAN preparation (from the young group). (a) Image of the raw SAN preparation. CT: crista terminalis; IVC: inferior vena cava; RA: right atrium; SEP: septum; SVC: superior vena cava. (b) Representative optical signals recorded at the leading pacemaking site. CL = cycle length. (c to h) Activation sequence over SAN from 0 to 9 ms. The area surrounded by yellow line in d is the leading pacemaker site which was harvested for further Western blot assay. Scale bar = 5 mm. (A color version of this figure is available in the online journal.)

activity or after pharmacological stimulation by iso-proterenol.[27] HCN2-deficient mice have similar mean heart rate to wild-type mice at rest and during spontaneous activity.[28] However, the intervals between successive heart beats of HCN2-deficient mice varied widely at rest and completely abolished during enhanced spontaneous activity and stimulation of cardiac β-adrenergic receptors by iso-proterenol or block of muscarinic receptors by atropine increased the heart rate. The HCN4-null mice as well as mice with a selective deletion of HCN4 in cardiomyocytes died between embryonic days 9.5 and 11.5. HCN4-deficient embryos have a slower heart rate than wild-type embryos and could not be stimulated by cAMP.[29] By contrast, HCN3-deficient mice display normal cardiac pacemaker activity with an abnormality in the ventricular repolarization.[30] In human, the physiological significance of HCN channel in the normal function of SAN has also been confirmed. Mutations in the HCN4 gene were found in patients with

congenital SSS, which suggests that a genetic defect in HCN channel can lead to SSS.[31,32] Currently, increasing evidence is highlighting that the HCN channel functions not only in the impulse formation but in the impulse propagation of SAN.[21,33] HCN1-deficient mouse have prolonged SACT. The prolonged SACT in HCN1$^{-/-}$ mice could result from a more negative maximal diastolic potential, which increases the distance to the threshold at which an action potential is generated. In this situation, more current and more time are required for a cell to charge the cell membrane of an adjacent cell to reach the threshold potential for an action potential and therefore slows the action potential conduction. This effect outweighs the competing effect of a more negative maximal diastolic potential to increase the availability of L-type Ca^{2+} channels and voltage-gated Na^+ channels. In the present study, we confirmed the contribution of HCN channels to the automaticity of the heart. Blockade of HCN channels with ivabradine prolonged CL
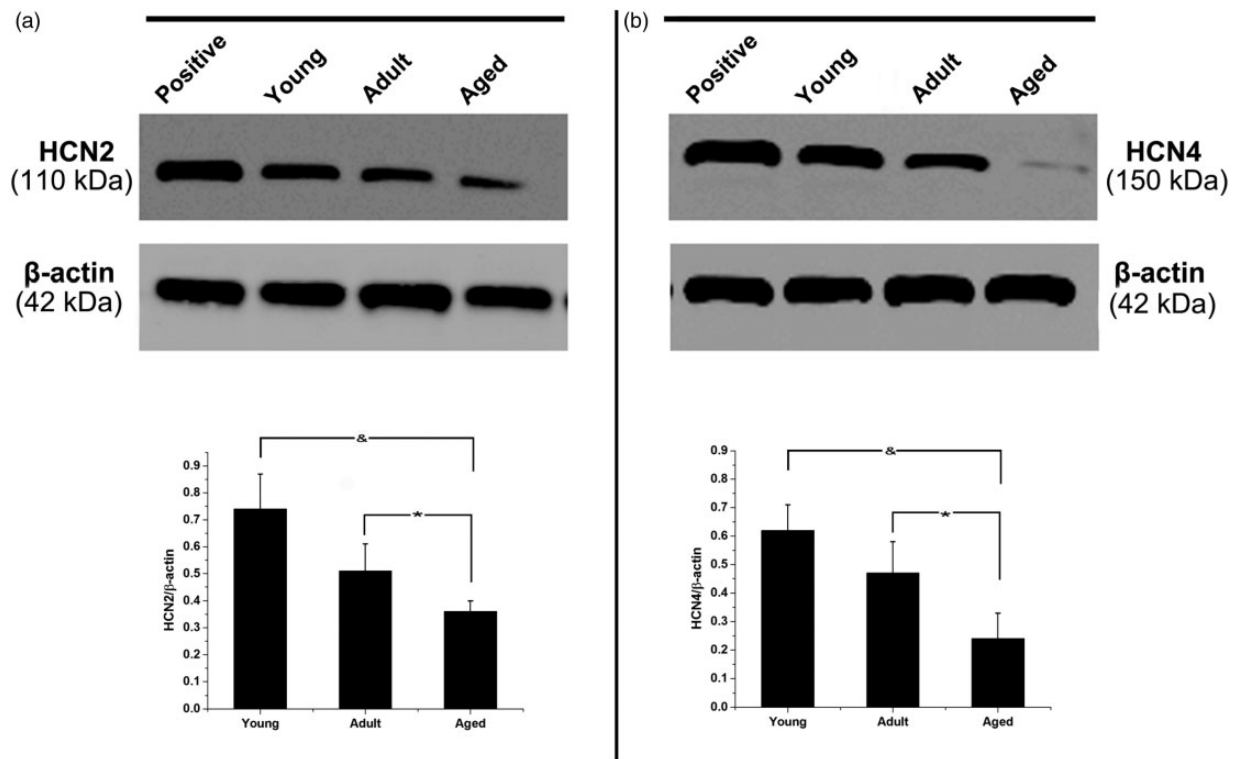
Figure 6 Western blot assays of HCN2 and HCN4 for each group. The HCN2 (a) and HCN4 (b) protein expression levels were reduced with aging. Membrane proteins of rat brain tissue were used as positive control. $^{\&}$indicates $p < 0.01$ versus the young group; * indicates $p < 0.05$ versus the adult group; n = 20 for each group

of all age groups in Langendorff hearts. Furthermore, we revealed the age-associated effect of ivabradine on CL, reflecting a compromised function of HCN channels in pacemaking during aging.

The heterogeneity of four HCN channel isoforms within the heart has been revealed. The transcripts of the HCN channel isoforms in the SAN were detected by different methods, including the RNAse protection assay, Northern blot analysis, *in situ* hybridization, quantitative polymerase chain reaction, and non-quantitative PCR. The HCN4 transcript is by far the most highly expressed in the SAN in adult rabbits, mice, and canines with lower levels of HCN2 and HCN1 transcripts.[12,13,34,35] This expression profile correlates well with findings in HCN knockout models. HCN4-knockout mice display a ~70% reduction in SAN I_f,[20] whereas deletion of HCN1 results in ~40% reduction and deletion of HCN2 results in ~30% reduction.[27,28] In human, HCN4 was also most abundant in SAN.[36] However, transcription is far away from functional ion channel protein. Due to the complex structure of SAN, little information is available as to the protein expression of the HCN channel isoforms in the SAN tissue, especially during aging. Functionally, the SAN can be divided into central and peripheral regions (central is adapted for pace-making only, whereas peripheral is adapted to protect the center and drive the atrial muscle as well as pacemaking).[37] Tellez *et al.* found that HCN1 and HCN4 mRNA were significantly more abundant in the rabbit SAN center than in both the SAN periphery and atrial muscle.[34] Our previous study revealed the presence of HCN2 and HCN4

transcripts in laser-captured rat SAN pacemaker cells from the central of SAN and their downregulated transcriptions with increased age. In the present study, we found HCN2 and HCN4 proteins in the rat SAN using immuno-fluorescence but failed to detect HCN1 and HCN3. The leading pacemaker site of the SAN tissue was identified by optical mapping for further Western blot analysis, which mainly consists of pacemaker cells within the central region of the SAN. In agreement with the functional results, Western blot analysis showed reduced expression of HCN2 and HCN4 proteins in the rat SAN during aging. Several studies also demonstrated a temporal and spatial expression of HCN channel isoforms during cardiac development. Yasui *et al.* showed that an extensive expression of HCN4 and an I_f current, similar to the I_f of adult SAN, is present in early embryonic mouse ventricular myocytes, which declined later on during the second half of embryonic development.[38] As reported by Schweizer *et al.*, transcriptions of HCN channel isoforms also varied in atrium, ventricle, and SAN during mouse cardiac development.[14] An investigation based on the overexpression of HCN2 channels in embryonic rat ventricular myocytes has shown a large increase of the rate of spontaneous activity correlated to the expression of pacemaker channels.[39] We speculate that reduction in I_f caused by declined HCN channel expression may at least in part involved in the lower IHR during aging. Further I_f patch clamp recording of single isolated SAN cells is needed.

Several agents were developed for their ability to selectively reduce heart rate act by a specific inhibition of HCN

channel; these substances have a potential for the treatment of diseases such as angina and heart failure. In the near future, new agents to focus on to facilitate the expression and function of HCN channel or devices based on the delivery of HCN channels *in situ*, or of a cellular source of HCN channels (biological pacemakers), will likely be developed for use in therapies for diseases of heart rhythm with the aim of replacing electronic pacemakers.

Conclusions

In summary, the expression of HCN channel isoforms may serve to maintain the physiological SAN pacemaker in rats. The aging-induced remodeling of HCN channel isoforms expression may be an important contributor to the declined SAN function in aging. Therapies that target HCN expression and/or HCN-based currents may be an interesting approach for treating age-related arrhythmias.

Authors' contributions: AM designed the study. XH and AM wrote the manuscript. PY, HZ and ZY researched and and analyzed the data.

REFERENCES

1. Gregoratos G. Permanent pacemakers in older persons. *J Am Geriatr Soc* 1999;**47**:1125–35
2. Schmidlin O, Bharati S, Lev M, Schwartz JB. Effects of physiological aging on cardiac electrophysiology in perfused Fischer 344 rat hearts. *Am J Physiol* 1992;**262**:H97–105
3. Alings AM, Bouman LN. Electrophysiology of the ageing rabbit and cat sinoatrial node—a comparative study. *Eur Heart J* 1993;**14**:1278–88
4. ME J. *Clinical cardiac electrophysiology: techniques and interpretations*, 2nd ed. Philadelphia: Lea and Febeger, 1993
5. Scicchitano P, Cortese F, Ricci G, Carbonara S, Moncelli M, Iacoviello M, Cecere A, Gesualdo M, Zito A, Caldarola P, Scrutinio D, Lagioia R, Riccioni G, Ciccone MM. Ivabradine, coronary artery disease, and heart failure: beyond rhythm control. *Drug Des Dev Ther* 2014;**8**:689–700
6. DiFrancesco D. Funny channel gene mutations associated with arrhythmias. *J Physiol* 2013;**591**:4117–24
7. Biel M, Schneider A, Wahl C. Cardiac HCN channels: structure, function, and modulation. *Trends Cardiovasc Med* 2002;**12**:206–12
8. Clapham DE. Not so funny anymore: pacing channels are cloned. *Neuron* 1998;**21**:5–7
9. Kaupp UB, Seifert R. Molecular diversity of pacemaker ion channels. *Annu Rev Physiol* 2001;**63**:235–57
10. Ludwig A, Zong X, Jeglitsch M, Hofmann F, Biel M. A family of hyperpolarization-activated mammalian cation channels. *Nature* 1998;**393**:587–91
11. Stieber J, Hofmann F, Ludwig A. Pacemaker channels and sinus node arrhythmia. *Trends Cardiovasc Med* 2004;**14**:23–8
12. Moosmang S, Stieber J, Zong X, Biel M, Hofmann F, Ludwig A. Cellular expression and functional characterization of four hyperpolarization-activated pacemaker channels in cardiac and neuronal tissues. *Eur J Biochem/FEBS* 2001;**268**:1646–52
13. Shi W, Wymore R, Yu H, Wu J, Wymore RT, Pan Z, Robinson RB, Dixon JE, McKinnon D, Cohen IS. Distribution and prevalence of hyperpolarization-activated cation channel (HCN) mRNA expression in cardiac tissues. *Circ Res* 1999;**85**:e1–6
14. Schweizer PA, Yampolsky P, Malik R, Thomas D, Zehelein J, Katus HA, Koenen M. Transcription profiling of HCN-channel isotypes throughout mouse cardiac development. *Basic Res Cardiol* 2009;**104**:621–9
15. Borlak J, Thum T. Hallmarks of ion channel gene expression in end-stage heart failure. *FASEB J* 2003;**17**:1592–608
16. Fernandez-Velasco M, Goren N, Benito G, Blanco-Rivero J, Bosca L, Delgado C. Regional distribution of hyperpolarization-activated current (If) and hyperpolarization-activated cyclic nucleotide-gated channel mRNA expression in ventricular cells from control and hypertrophied rat hearts. *J Physiol* 2003;**553**:395–405
17. Strauss HC, Saroff AL, Bigger JT Jr, Giardina EG. Premature atrial stimulation as a key to the understanding of sinoatrial conduction in man. Presentation of data and critical review of the literature. *Circulation* 1973;**47**:86–93
18. Breithardt G, Seipel L, Loogen F. Sinus node recovery time and calculated sinoatrial conduction time in normal subjects and patients with sinus node dysfunction. *Circulation* 1977;**56**:43–50
19. Safa-Tisseront V, Ponchon P, Laude D, Elghozi JL. Contribution of the autonomic nervous system to blood pressure and heart rate variability changes in early experimental hyperthyroidism. *Eur J Pharmacol* 1998;**352**:247–55
20. Maier SK, Westenbroek RE, Yamanushi TT, Dobrzynski H, Boyett MR, Catterall WA, Scheuer T. An unexpected requirement for brain-type sodium channels for control of heart rate in the mouse sinoatrial node. *Proc Natl Acad Sci USA* 2003;**100**:3507–12
21. Bois P, Bescond J, Renaudon B, Lenfant J. Mode of action of bradycardic agent, S 16257, on ionic currents of rabbit sinoatrial node cells. *Br J Pharmacol* 1996;**118**:1051–7
22. Huang X, Yang P, Du Y, Zhang J, Ma A. Age-related down-regulation of HCN channels in rat sinoatrial node. *Basic Res Cardiol* 2007;**102**:429–35
23. Jia B, Choy E, Cote G, Harmon D, Ye S, Kan Q, Mankin H, Hornicek F, Duan Z. Cyclin-dependent kinase 11 (CDK11) is crucial in the growth of liposarcoma cells. *Cancer Lett* 2014;**342**:104–12
24. DiFrancesco D. Pacemaker mechanisms in cardiac tissue. *Annu Rev Physiol* 1993;**55**:455–72
25. Robinson RB, Siegelbaum SA. Hyperpolarization-activated cation currents: from molecules to physiological function. *Annu Rev Physiol* 2003;**65**:453–80
26. Baruscotti M, Bucchi A, Viscomi C, Mandelli G, Consalez G, Gnecchi-Rusconi T, Montano N, Casali KR, Micheloni S, Barbuti A, DiFrancesco D. Deep bradycardia and heart block caused by inducible cardiac-specific knockout of the pacemaker channel gene Hcn4. *Proc Natl Acad Sci USA* 2011;**108**:1705–10
27. Fenske S, Krause SC, Hassan SI, Becirovic E, Auer F, Bernard R, Kupatt C, Lange P, Ziegler T, Wotjak CT, Zhang H, Hammelmann V, Paparizos C, Biel M, Wahl-Schott CA. Sick sinus syndrome in HCN1-deficient mice. *Circulation* 2013;**128**:2585–94
28. Ludwig A, Budde T, Stieber J, Moosmang S, Wahl C, Holthoff K, Langebartels A, Wotjak C, Munsch T, Zong X, Feil S, Feil R, Lancel M, Chien KR, Konnerth A, Pape HC, Biel M, Hofmann F. Absence epilepsy and sinus dysrhythmia in mice lacking the pacemaker channel HCN2. *EMBO J* 2003;**22**:216–24
29. Stieber J, Herrmann S, Feil S, Loster J, Feil R, Biel M, Hofmann F, Ludwig A. The hyperpolarization-activated channel HCN4 is required for the generation of pacemaker action potentials in the embryonic heart. *Proc Natl Acad Sci USA* 2003;**100**:15235–40

30. Fenske S, Mader R, Scharr A, Paparizos C, Cao-Ehlker X, Michalakis S, Shaltiel L, Weidinger M, Stieber J, Feil S, Feil R, Hofmann F, Wahl-Schott C, Biel M. HCN3 contributes to the ventricular action potential waveform in the murine heart. *Circ Res* 2011;**109**:1015–23

31. Milanesi R, Baruscotti M, Gnecchi-Ruscone T, DiFrancesco D. Familial sinus bradycardia associated with a mutation in the cardiac pacemaker channel. *New Engl J Med* 2006;**354**:151–7

32. Schulze-Bahr E, Neu A, Friederich P, Kaupp UB, Breithardt G, Pongs O, Isbrandt D. Pacemaker channel dysfunction in a patient with sinus node disease. *J Clin Invest* 2003;**111**:1537–45

33. Wahl-Schott C, Fenske S, Biel M. HCN channels: new roles in sinoatrial node function. *Curr Opin Pharmacol* 2014;**15**:83–90

34. Tellez JO, Dobrzynski H, Greener ID, Graham GM, Laing E, Honjo H, Hubbard SJ, Boyett MR, Billeter R. Differential expression of ion channel transcripts in atrial muscle and sinoatrial node in rabbit. *Circ Res* 2006;**99**:1384–93

35. Zicha S, Fernandez-Velasco M, Lonardo G, L'Heureux N, Nattel S. Sinus node dysfunction and hyperpolarization-activated (HCN) channel subunit remodeling in a canine heart failure model. *Cardiovasc Res* 2005;**66**:472–81

36. Dobrzynski H, Boyett MR, Anderson RH. New insights into pacemaker activity: promoting understanding of sick sinus syndrome. *Circulation* 2007;**115**:1921–32

37. Boyett MR, Dobrzynski H, Lancaster MK, Jones SA, Honjo H, Kodama I. Sophisticated architecture is required for the sinoatrial node to perform its normal pacemaker function. *J Cardiovasc Electrophysiol* 2003;**14**:104–6

38. Yasui K, Liu W, Opthof T, Kada K, Lee JK, Kamiya K, Kodama I. I(f) current and spontaneous activity in mouse embryonic ventricular myocytes. *Circ Res* 2001;**88**:536–42

39. Qu J, Barbuti A, Protas L, Santoro B, Cohen IS, Robinson RB. HCN2 overexpression in newborn and adult ventricular myocytes: distinct effects on gating and excitability. *Circ Res* 2001;**89**:E8–14